Luoqiang Liu, Xing Zhang, Lingling Zhu*, Yazhu Wei, Chao Guo and Hongxia Li

Preparation of hexagonal micro-sized α-Al_2O_3 platelets from a milled $Al(OH)_3$ precursor with NH_4F and NH_4Cl additives

https://doi.org/10.1515/znb-2019-0080
Received April 5, 2019; accepted June 23, 2019

Abstract: Hexagonal α-Al_2O_3 platelets with about 1-μm diameter and 0.2-μm thickness are prepared by the calcination of a milled $Al(OH)_3$ precursor with NH_4F and NH_4Cl additives. The influences of the ball milling treatment and the composite additive on the microstructure of α-Al_2O_3 micro-powders are studied. The results indicate that the particle size distribution of α-Al_2O_3 is highly dependent on the aggregate size of the $Al(OH)_3$ precursor and that the morphology of α-Al_2O_3 can be significantly favored by the addition of 5 wt.% NH_4F and 5 wt.% NH_4Cl as additives. The growth velocity of the (0001) plane is significantly reduced because of the accelerated growth rate of other crystal faces caused by the increase of gas phase mass transfer. The combined effect of composite additives and precursor ball milling treatment leads to the generation of well-developed α-Al_2O_3 platelets with uniform size distribution.

Keywords: ammonium halide additives; hexagonal α-Al_2O_3 platelets; milled $Al(OH)_3$ precursors.

1 Introduction

Plate-like α-Al_2O_3 powders have been widely applied in the fields of high-strength ceramics, abrasives and other refractory materials owing to its excellent properties including good chemical stability, high elastic modulus as well as high tensile and compression strength [1–7].

***Corresponding author: Lingling Zhu,** School of Materials Science and Engineering, Zhengzhou University, Zhengzhou 450001, P.R. China; and State Key Laboratory of Advanced Refractories of China, Sinosteel Luoyang Institute of Refractories Research Co., Luoyang 471039, P.R. China, e-mail: llzhu@zzu.edu.cn
Luoqiang Liu, Xing Zhang, Yazhu Wei and Chao Guo: School of Materials Science and Engineering, Zhengzhou University, Zhengzhou 450001, P.R. China
Hongxia Li: State Key Laboratory of Advanced Refractories of China, Sinosteel Luoyang Institute of Refractories Research Co., Luoyang 471039, P.R. China

Until now, many methods have been developed to synthesize α-Al_2O_3 platelets [8–10], such as the melt salt method [11], hydrothermal synthesis [12], laser scanning [13], electrostatic spray-assisted chemical vapor deposition [14] and high-temperature calcination [15]. As the crystal growth of α-Al_2O_3 is mainly determined by the relative growth rates of various crystal faces, not only the internal structural factors but also the external conditions [16–18], such as the type of precursor, the reaction temperature and the addition of crystal seeds (including α-Al_2O_3, α-Fe_2O_3, α-Cr_2O_3, etc.), have been considered to control the morphology of α-Al_2O_3 powders.

In particular, it has been demonstrated that the type and microstructure (morphology, aggregate size and shape) of the precursor are crucial to control the morphology of α-Al_2O_3 powders [19, 20]. As the larger-sized precursor aggregates could be broken into highly active fragments under high-energy ball milling, the neck growth of α-Al_2O_3 during calcination could be efficiently suppressed, and almost-spherical α-Al_2O_3 powders of ~1.0-μm size were synthesized by the calcination of the ground precursor at 1450°C [21]. Moreover, although many kinds of additives [15, 22–24], such as AlF_3, ZnF_2, NH_4F, etc., have been introduced to improve the α-phase transformation and the morphology of α-Al_2O_3, the effect of fluoride additives on the morphology modification of α-Al_2O_3 particles is different, depending on the precursor [20].

Therefore, considering the above aspects, in current technology, commercial $Al(OH)_3$ with spherical agglomerates and about 100-μm size is ball milled as the precursor for the preparation of α-Al_2O_3. Composite additives (NH_4F and NH_4Cl) are introduced to modify the α-Al_2O_3 microstructure. In the present work, hexagonal α-Al_2O_3 micro-platelets with a uniform distribution are prepared by high-temperature calcination, and the growth process is discussed.

2 Experimental procedure

The preparation of α-Al_2O_3 powders from a commercial $Al(OH)_3$ precursor (Shandong Branch of CHACLO, China)

was carried out in the following way. First, ball milling treatment of commercial $Al(OH)_3$ precursor was carried out for 9 h in a batch-type planetary mill (ND7-2L, Nanjing LAB Industrial Co., Ltd., China) with zirconia balls using ethanol as the dispersion medium. The ratio of grinding balls to material was 15:1 in weight, and a rotational speed of 240 r min^{-1} was employed in the experiments. The milled $Al(OH)_3$ samples were oven dried at $T = 80°C$ for 24 h. Then, 5 wt.% NH_4F (Sinopharm Chemical Reagent Beijing Co., Ltd., China) and 5 wt.% NH_4Cl (Sinopharm Chemical Reagent Beijing Co., Ltd., China) additives were introduced into the milled $Al(OH)_3$ precursor, and the mixture was ground in an agate mortar for 1 h. Finally, the commercial $Al(OH)_3$ precursor, the $Al(OH)_3$ precursor milled for 9 h and the milled $Al(OH)_3$ precursor with 5 wt.% NH_4F and 5 wt.% NH_4Cl as additives were calcined separately at $T = 1300°C$ for 3 h for comparison.

The phase compositions and the crystallinity of the samples after milling and calcination were identified by powder X-ray diffraction (XRD; X′ Pert Pro MPD, Philips, Eindhoven, Netherlands) with Cu$K\alpha$ radiation (λ =0.154 nm, 40 kV, 40 mA) in the 2θ range 20–80° and with a scan rate of 5° min^{-1}. Fourier transform infrared (FTIR; Tensor II, Bruker) spectra of the α-Al_2O_3 samples were collected between 4000 and 400 cm^{-1} on a Tensor 37 infrared spectrometer with a wavenumber resolution of 4 cm^{-1}. The microstructure of the milled and unmilled $Al(OH)_3$ samples was analyzed by cold field emission scanning electron microscopy (SEM; JSM-7500F, JEOL, Tokyo, Japan) at an accelerating voltage of 15 kV, and the morphology evolution of the α-Al_2O_3 samples upon calcination at $T = 1300°C$ was observed by field emission SEM (Sigma HD, Zeiss, Oberkochen, Germany) at an accelerating voltage of 10 kV.

3 Results and discussion

The effect of the ball milling treatment on the phase composition and crystallinity of the precursor is shown in Fig. 1. The XRD patterns of the commercial samples and those milled for 9 h indicate that the crystallinity of the precursor could be significantly decreased by the ball milling treatment, because the diffraction peaks (shown in the XRD pattern of the 9-h milled precursor) related to gibbsite (JCPDS File No: 74-1775) are weakened and broadened after 9 h of ball milling. In particular, the peak centered at 68.88º corresponding to the 026 reflection of gibbsite even disappears. These results demonstrate that the 9-h ball milling treatment results in a grain refinement and

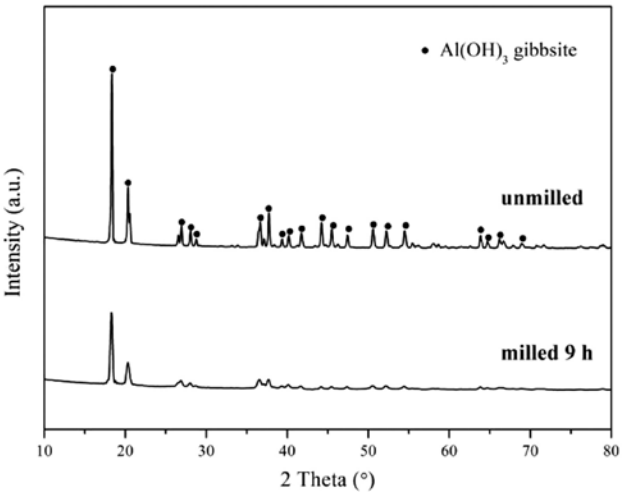

Fig. 1: XRD patterns of the $Al(OH)_3$ precursors before and after ball milling.

poor crystallinity of the $Al(OH)_3$ precursor [25], although the milled and unmilled $Al(OH)_3$ precursors are identical in phase composition.

Figure 2 presents the microstructure of the commercial $Al(OH)_3$ precursor. It is seen that the $Al(OH)_3$ precursor without ball milling consists mainly of spherical agglomerates in the size range of 100–200 μm (as shown in Fig. 2a), which consist of many smaller-sized grains (as shown in Fig. 2b). In comparison, the morphology of the ball-milled $Al(OH)_3$ precursor shown in Fig. 3 indicates that these large agglomerates are mostly broken into irregularly shaped particles in the size range of ≤5 μm by 9-h ball milling, accompanied by a formation of a small amount of irregular pieces in the size range of 10–30 μm. The above results reveal that the ball milling treatment leads to a significant refinement in morphology and particle size distribution of the $Al(OH)_3$ precursor.

Figure 4 shows the XRD patterns of the samples obtained by calcination of the commercial $Al(OH)_3$ precursor, the 9-h ball-milled $Al(OH)_3$ precursor and the milled $Al(OH)_3$ precursor with 5 wt.% NH_4F and 5 wt.% NH_4Cl additives at 1300°C for 3 h. The characteristic peaks at 25.590º, 35.155º, 37.781º, 43.353º, 52.561º, 57.504º, 61.310º, 66.530º, 68.215º and 76.883º corresponding to the 012, 104, 110, 113, 024, 116, 018, 214, 300 and 1010 reflections of α-Al_2O_3, respectively [15], confirm that single-phase α-Al_2O_3 could be synthesized by the calcination at $T = 1300°C$.

To further prove the above result, these calcined samples were analyzed by FTIR. As shown in Fig. 5, intense bands between 1000 and 400 cm^{-1} assigned to the Al–O–Al stretching emerge in the spectra [26], while the peaks at 688, 641, 595, 493, 469 and 453 cm^{-1} result

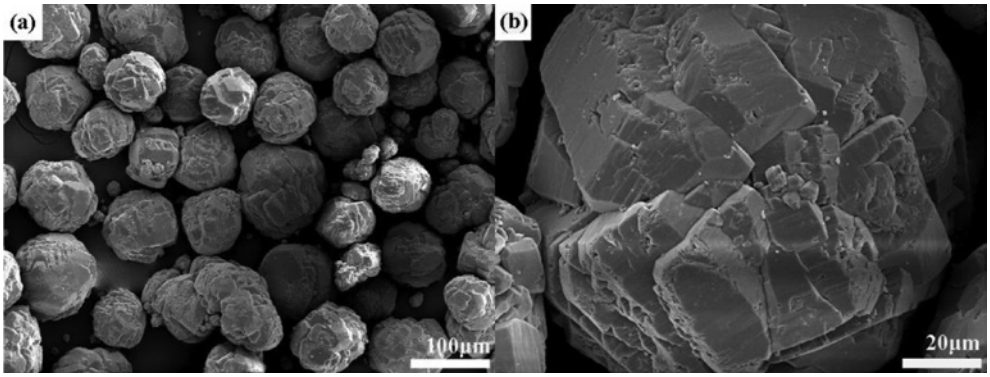

Fig. 2: SEM photographs of the commercial $Al(OH)_3$ precursor. Picture (b) is the magnification of the selected area in picture (a).

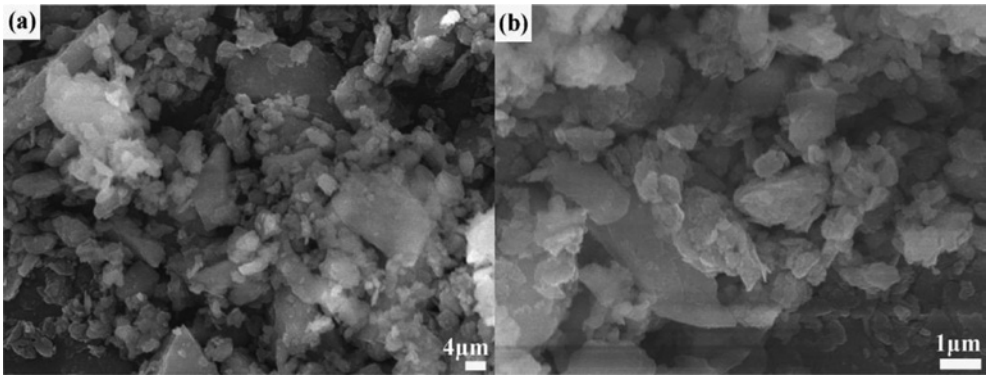

Fig. 3: SEM photographs of the $Al(OH)_3$ precursor after 9 h of ball milling. Picture (b) is the magnification of the selected area in picture (a).

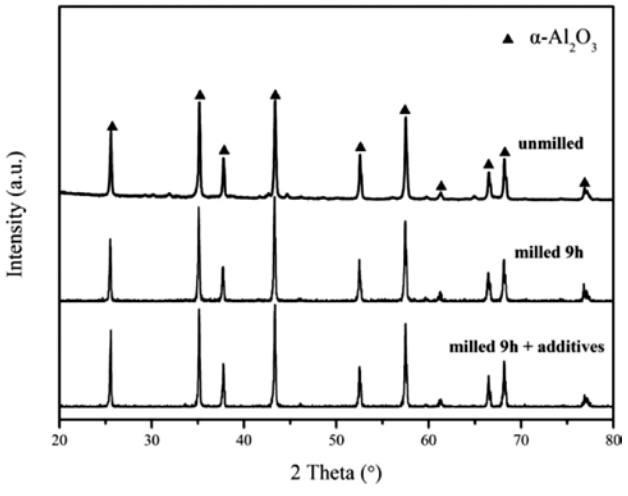

Fig. 4: XRD patterns of samples obtained by calcination at $T=1300°C$.

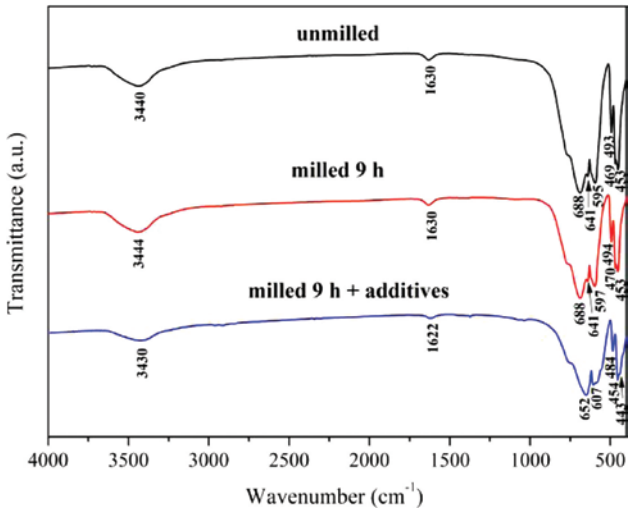

Fig. 5: FTIR spectra of samples obtained by calcination at $T=1300°C$.

from the vibrations of Al–O bonds of the AlO_6 units [21]. The FTIR results confirm that the samples calcined at $T=1300°C$ are composed of α-Al_2O_3.

The morphological evolution of the α-Al_2O_3 samples can be followed in Figs. 6–8, which present SEM photographs of the α-Al_2O_3 prepared by the calcination of commercial $Al(OH)_3$, 9-h ball-milled $Al(OH)_3$ and 9-h ball-milled $Al(OH)_3$ with NH_4F and NH_4Cl additives at 1300°C, respectively. As shown in Fig. 6a, the α-Al_2O_3 particles obtained from the commercial $Al(OH)_3$ precursor

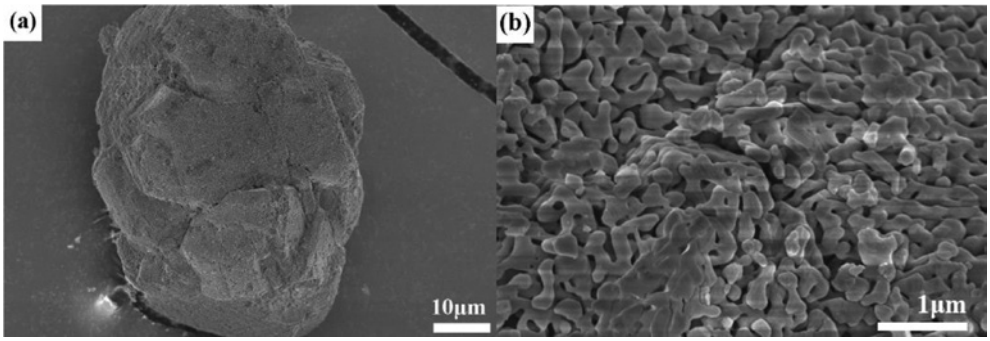

Fig. 6: SEM photographs of the α-Al_2O_3 sample obtained by the calcination of commercial $Al(OH)_3$ at $T=1300°C$ for 3 h. Picture (b) is the magnification of the selected area in picture (a).

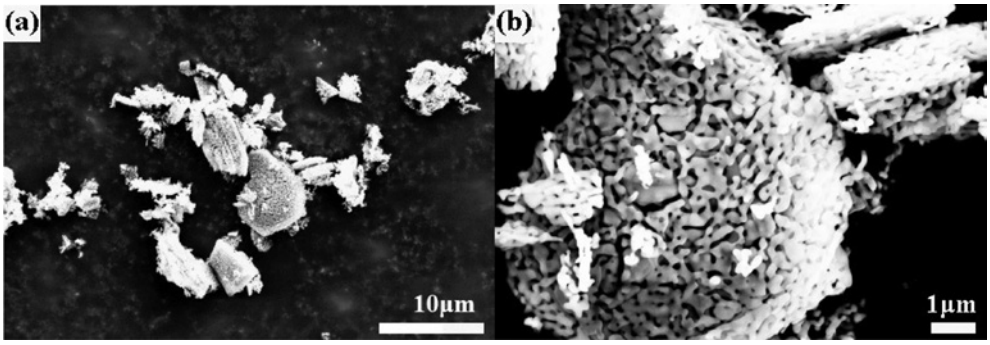

Fig. 7: SEM photographs of the α-Al_2O_3 sample obtained by the calcination of 9-h ball-milled $Al(OH)_3$ at $T=1300°C$ for 3 h. Picture (b) is the magnification of the selected area in picture (a).

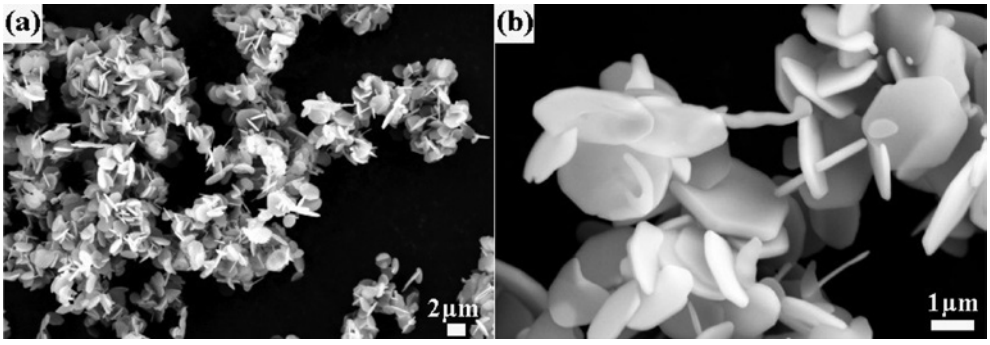

Fig. 8: SEM photographs of the α-Al_2O_3 sample obtained by the calcination of 9-h ball-milled $Al(OH)_3$ containing NH_4F and NH_4Cl additives. Picture (b) is the magnification of the selected area in picture (a).

fired at 1300°C maintain the initial aggregate shape with a worm-like structure formed by the neck growth of α-Al_2O_3 grains. By comparing Fig. 7 with Fig. 6, it is seen that the aggregate size has been significantly decreased due to the morphology refinement of the milled $Al(OH)_3$ (see Fig. 2). The above results indicate that the α-Al_2O_3 powders obtained by the calcination of the unmilled and milled $Al(OH)_3$ precursors at 1300°C have similar worm-like microstructures because the formation of the as-synthesized α-Al_2O_3 mainly follows the solid phase mass transfer mechanism [27].

In contrast, α-Al_2O_3 powders obtained from the milled $Al(OH)_3$ precursor with the 5 wt.% NH_4Cl and 5 wt.% NH_4F additives exhibit a well-defined hexagonal platelet morphology as shown in Fig. 8. The diameters of the α-Al_2O_3 platelets are about 1 μm, and the thicknesses are about 200 nm. It can be seen that the introduction of the NH_4Cl and NH_4F additives results in a significant morphological modification of the α-Al_2O_3 powders from the milled $Al(OH)_3$ precursor calcined at $T=1300°C$.

The phenomenon suggests that the formation of hexagonal α-Al_2O_3 platelets is highly related to the addition of

NH_4Cl and NH_4F, because the additives cause a different growth rate along the respective crystal axis and consequently influence the microstructure of α-Al_2O_3. Previous studies have reported [9, 28, 29] that the (0001) surface is the most stable surface of α-Al_2O_3 and appears predominantly, thereby promoting the formation of hexagonal platelets. In the present study, the addition of NH_4Cl and NH_4F accelerates gas phase mass transport with formation of gaseous intermediates including mainly AlOF and AlOCl, etc. [23, 30], and hence promotes the growth rate of α-Al_2O_3 along the crystal orientation $(10\bar{1}0)$. As a result, the growth velocity of the $(10\bar{1}0)$ crystal faces is significantly increased, and the growth velocity of the (0001) plane is greatly reduced in the presence of NH_4Cl and NH_4F. Thus, the α-Al_2O_3 powders prepared by calcination of the milled $Al(OH)_3$ precursor with NH_4Cl and NH_4F additives appear as well-developed hexagonal platelets.

4 Summary

Well-shaped hexagonal α-Al_2O_3 platelets of ~1.0-μm diameter and ~0.2-μm thickness have been synthesized from a ball-milled $Al(OH)_3$ precursor with NH_4Cl and NH_4F additives calcined at 1300°C. As spherical $Al(OH)_3$ agglomerates in the size range of 100–200 μm are mostly broken into irregularly shaped particles in the ≤5 μm size range, the size distribution of α-Al_2O_3 powders is significantly improved through the incorporation of the morphology refinement of the precursor caused by the ball milling treatment. Moreover, the growth velocity of the (0001) plane could be reduced by the introduction of NH_4Cl and NH_4F additives, because the growth of α-Al_2O_3 crystals along $(10\bar{1}0)$ is greatly promoted by gaseous AlOF and AlOCl or other intermediates. Therefore, the addition of NH_4Cl and NH_4F appears to be helpful in the generation of α-Al_2O_3 platelets.

Acknowledgments: The authors acknowledge the National Natural Science Foundation of China (contract no. U1504526), the Key Scientific Research Project for Universities and Colleges in Henan Province (contract no. 19A430028) and the Open Foundation of the State Key Laboratory of Refractories and Metallurgy (G201909) for financial support.

References

[1] Y. H. Huang, Y. Xia, S. Liao, Z. F. Tong, G. Liu, Y. Li, Z. P. Chen, *Ceram. Int.* **2014**, *40*, 8071.
[2] Y. Q. Wu, Y. F. Zhang, X. X. Huang, J. K. Guo, *Ceram. Int.* **2001**, *27*, 265.
[3] W. J. Gu, L. L. Zhu, X. J. Shang, D. F. Ding, L. Q. Liu, G. L. Chen, G. T. Ye, *J. Alloys Compd.* **2019**, *772*, 637.
[4] J. Ding, C. Yu, J. P. Liu, C. J. Deng, H. X. Zhu, *Mater. Chem. Phys.* **2018**, *206*, 193.
[5] S. S. Li, J. H. Liu, J. K. Wang, L. Han, H. J. Zhang, S. W. Zhang, *Ceram. Int.* **2018**, *44*, 12940.
[6] A. Huang, Y. J. Wang, Y. S. Zou, H. Z. Gu, L. P. Fu, *Ceram. Int.* **2018**, *44*, 14617.
[7] Y. Li, L. L. Zhu, K. Liu, D. F. Ding, J, Zhang, G. T. Ye, *Ceram. Int.* **2019**, *45*, 12066.
[8] X. H. Jin, L. Gao, *J. Am. Ceram. Soc.* **2004**, *87*, 533.
[9] W. L. Wang, J. Q. Bi, Y. Q. Qi, Z. Zhang, Z. Xing, H. L. Zhu, Y. J. Bai, *Powder Technol.* **2010**, *201*, 273.
[10] Y. F. Chang, J. Wu, M. M. Zhang, E. Kupp, G. L. Messing, *Ceram. Int.* **2017**, *43*, 12684.
[11] L. H. Zhu, R. R. Tu, Q. W. Huang, *Ceram. Int.* **2012**, *38*, 901.
[12] W. L. Suchanek, J. M. Garcés, P. F. Fulvio, M. Jaroniec, *Chem. Mater.* **2010**, *22*, 6564.
[13] Y. Q. Wu, K. L. Choy, L. L. Hench, *J. Am. Ceram. Soc.* **2004**, *87*, 3.
[14] M. Wei, D. Zhi, K. L. Choy, *Nanotechnology* **2006**, *17*, 181.
[15] L. L. Zhu, C. H. Sun, L. G. Chen, X. F. Lu, S. Li, G. T. Ye, L. Q. Liu, *Z. Naturforsch.* **2017**, *72b*, 665.
[16] H. I. Hsiang, C. C. Chuang, T. H. Chen, F. S. Yen, *Ceram. Int.* **2010**, *36*, 1467.
[17] M. M. Zhang, Y. F. Chang, N. Pulati, S. T. Zhang, Y. Sun, J. Wu, Y. C. Liu, B. Yang, W. W. Cao, *Mater. Lett.* **2018**, *210*, 182.
[18] K. L. Gavrilov, S. J. Bennison, K. R. Mikeska, R. Levi-Setti, *J. Mater. Sci.* **2003**, *38*, 3965.
[19] H. J. Kim, T. G. Kim, J. J. Kim, S. S. Park, S. S. Hong, G. D. Lee, *J. Phys. Chem. Solids* **2008**, *69*, 1521.
[20] H. Chen, Q. D. Wu, T. X. Yang, M. Q. Li, H. C. Xie, C. Lin, *Ceram. Int.* **2015**, *41*, 12288.
[21] S. Li, L. L. Zhu, L. Q. Liu, L. G. Chen, H. X. Li, C. H. Sun, *Z. Naturforsch.* **2018**, *73b*, 589.
[22] J. Li, Y. S. Wu, Y. B. Pan, W. B. Liu, J. K. Guo, *Ceram. Int.* **2007**, *33*, 919.
[23] H. S. Kim, N. K. Park, T. J. Lee, M. Kang, *Ceram. Int.* **2014**, *40*, 3813.
[24] F. Mirjalili, *Bull. Mater. Sci.* **2014**, *37*, 1709.
[25] Z. J. Liu, W. C. Wang, D. Z. Yang, S. Wang, L. Y. Dai, Z. L. Yang, *Ceram. Int.* **2015**, *42*, 3411.
[26] X. L. Du, Y. Q. Wang, X. H. Su, J. G. Li, *Powder Technol.* **2009**, *192*, 40.
[27] D. Riello, C. Zetterström, C. Parr, M. A. L. Braulio, M. Moreira, J. B. Gallo, V. C. Pandolfelli, *Ceram. Int.* **2016**, *42*, 9804.
[28] B. Hinnemann, E. A. Carter, *J. Phys. Chem. C.* **2007**, *111*, 7105.
[29] N. G. Petrik, P. L. Huestis, J. A. LaVerne, A. B. Aleksandrov, T. M. Orlando, G. A. Kimmel, *J. Phys. Chem. C* **2018**, *122*, 9540.
[30] P. F. Tan, J. Müller, D. Neuschütz, *J. Electrochem. Soc.* **2005**, *152*, C288.